Use of thiol-disulfide equilibria to measure the energetics of assembly of transmembrane helices in phospholipid bilayers

Lidia Cristian, James D. Lear†, and William F. DeGrado†

Department of Biochemistry and Biophysics, School of Medicine, University of Pennsylvania, Philadelphia, PA 19104-6059

Communicated by James A. Wells, Sunesis Pharmaceuticals, Inc., South San Francisco, CA, October 17, 2003 (received for review May 25, 2003)

Despite significant efforts and promising progress, the understanding of membrane protein folding lags behind that of soluble proteins. Insights into the energetics of membrane protein folding have been gained from biophysical studies in membrane-mimicking environments (primarily detergent micelles). However, the development of techniques for studying the thermodynamics of folding in phospholipid bilayers remains a considerable challenge. We had previously used thiol-disulfide exchange to study the thermodynamics of association of transmembrane α-helices in detergent micelles; here, we extend this methodology to phospholipid bilayers. The system for this study is the homotetrameric M2 proton channel protein from the influenza A virus. Transmembrane peptides from this protein specifically self-assemble into tetramers that retain the ability to bind to the drug amantadine. Thiol-disulfide exchange under equilibrium conditions was used to quantitatively measure the thermodynamics of this folding interaction in phospholipid bilayers. The effects of phospholipid acyl chain length and cholesterol on the peptide association were investigated. The association of the helices strongly depends on the thickness of the bilayer and cholesterol levels present in the phospholipid bilayer. The most favorable folding occurred when there was a good match between the width of the apolar region of the bilayer and the hydrophobic length of the transmembrane helix. Physiologically relevant variations in the cholesterol level are sufficient to strongly influence the association. Evaluation of the energetics of peptide association in the presence and absence of cholesterol showed a significantly tighter association upon inclusion of cholesterol in the lipid bilayers.

In contrast to the substantial literature dealing with the structural energetics of water-soluble proteins, relatively little is known about the forces that determine the stability of membrane proteins (1). The understanding of helical membrane protein folding has been complicated by the difficulties associated with structure determination and thermodynamic characterization of membrane proteins. Compared with water-soluble proteins, relatively few membrane protein structures are known at atomic resolution, although new structures are beginning to appear more rapidly (1–8). Thermodynamic analysis of membrane proteins has been hampered by the experimental difficulties imposed by their insolubility in water and great stability in membranes. Thus, to understand folding of membrane proteins it is essential to discover systems in which folding is in thermodynamic equilibrium and to develop methods to quantitatively assess this equilibrium in membrane-like environments. Several biophysical techniques have been intensively used in thermodynamic studies of membrane protein association in detergent systems (9–15). However, the ideal environment for studying membrane proteins is the lipid bilayer because lipids mimic more closely the native membrane environment. Thus, there is considerable interest in finding reversible conditions under which the thermodynamics of membrane protein association can be studied in these environments.

Recently, we have reported a disulfide-coupled folding approach to measure the energetics of transmembrane protein association in detergent micelles (16). The reversible association of a transmembrane peptide in micelles was measured by quantitatively assessing the extent of disulfide formation under reversible redox conditions with a thiol-disulfide buffer. Here, we describe the application of the disulfide-coupled folding method to measure the energetics of transmembrane peptide association in phospholipid bilayers. The 19–46 transmembrane fragment of the M2 protein from influenza A virus ($M2TM_{19-46}$) was used as a model membrane protein for this study. M2 is a small homotetrameric proton channel, consisting of 97-residue monomers (17–19). The protein has two cysteine residues at positions 17 and 19 at the extracellular domain, which form a mixture of covalent dimers and tetramers (17). The active oligomeric form of M2 is homotetrameric (20). Proton channel activity has been reported in lipid bilayers from a synthetic protein containing the predicted transmembrane region of M2 (21), suggesting that the channel-forming properties of the full-length protein reside in its transmembrane region. CD and solid-state NMR studies showed that the transmembrane segment of M2 adopts an α-helical structure in bilayers (22, 23), is oligomeric in bilayers (24), and reversibly associates into tetramers in detergent micelles (16, 25, 26). A peptide from residues 19–46 contains a single native Cys residue, which reversibly forms intermolecular disulfides in the tetramer (16). Hence, this peptide has proven to be a very good candidate for thermodynamic studies in micelles by thiol-disulfide interchange. Here, we investigate the ability of this peptide to associate in phospholipid bilayers and determine the effects of membrane thickness and added cholesterol on the equilibrium of association.

Materials and Methods

Peptide Synthesis and Sample Preparation. $M2TM_{19-46}$ peptide was synthesized and purified as described (16). Small unilamellar vesicles were prepared by codissolving $M2TM_{19-46}$/trifluoroethanol stock solutions with the appropriate amount of phospholipid from a stock solution in ethanol. The solvent was evaporated under a stream of nitrogen, and the protein/phospholipid film was kept overnight under high vacuum to remove all traces of solvent. The dry peptide/phospholipid films obtained were then hydrated in buffer (0.1 M Tris·HCl/0.2 M KCl/1 mM EDTA, pH 8.6), vortexed, and sonicated to clarity by using a bath sonicator (Laboratory Supplies, Hicksville, NY). The concentration of peptide (20 μM) was kept constant while varying the phospholipid concentration to attain the desired peptide/phospholipid mole ratios (typically between 1:100 and 1:1,500). The phospholipids used in this study were: 1-palmitoyl-2-oleoyl-*sn*-glycero-3-phosphocholine (POPC), 1,2-dilauroyl-*sn*-

Abbreviations: POPC, 1-palmitoyl-2-oleoyl-*sn*-glycero-3-phosphocholine; DLPC, 1,2-dilauroyl-*sn*-glycero-3-phosphocholine; DMPC, 1,2-dimyristoyl-*sn*-glycero-3-phosphocholine; GSH, glutathione; GSSG, oxidized glutathione.

†To whom correspondence should be addressed. E-mail: lear@mail.med.upenn.edu or wdegrado@mail.med.upenn.edu.

www.pnas.org/cgi/doi/10.1073/pnas.2536751100

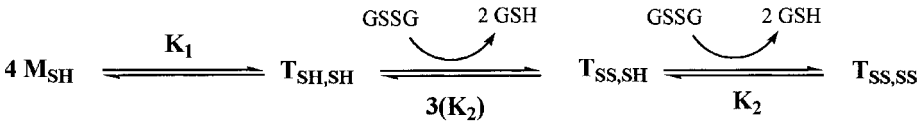

Scheme 1. Thermodynamic coupling between disulfide formation and tetramerization.

glycero-3-phosphocholine (DLPC), and 1,2-dimyristoyl-*sn*-glycero-3-phosphocholine (DMPC). All lipids were purchased from Avanti Polar Lipids.

Incorporation of amantadine into the peptide/phospholipid samples was carried out by first adding the desired amount of amantadine from a trifluoroethanol stock solution to a glass vial and evaporating the solvent under a stream of nitrogen. The peptide was then incorporated into DLPC at a peptide/phospholipid mole ratio of 1:1,500 as described above; the samples were hydrated in buffer, sonicated to clarity, and then added to the amantadine films. Reversible disulfide formation was initiated by adding oxidized glutathione (GSSG) and reduced glutathione (GSH) at varying ratios to the samples. The final molar ratios of peptide/DLPC/amantadine were 1:1,500:5, 1:1,500:15, and 1:1,500:50.

For samples containing cholesterol, mixtures of peptide, lipid, and the desired mol percentage of cholesterol (relative to lipid concentration) were codissolved from trifluoroethanol or ethanol stock solutions, dried under nitrogen, and kept under high vacuum overnight. The dry films were then hydrated in buffer and sonicated to clarity in a bath sonicator.

CD. CD measurements were performed on an Aviv Associates (Lakewood, NJ) 62A DS CD spectrometer at 25°C. $M2TM_{19-46}$ was incorporated into DLPC, DMPC, and POPC vesicles at a ratio of 1:500 as described above. The buffer was 50 mM Tris·HCl/0.1 M NaCl, pH 8.0. CD spectra were recorded in a 0.1-cm quartz cell, and data were collected as an average of three scans by using a wavelength step of 1 nm. Background spectra (phospholipids plus buffer) were subtracted from the peptide/phospholipid CD spectra.

Thiol-Disulfide Exchange Equilibria with GSH Redox Buffer. Thiol-disulfide exchange reactions of $M2TM_{19-46}$ incorporated into phospholipid vesicles were carried out with the same procedure used with detergent micelles, as described (16). The time required for the equilibration of the samples was 5 h as determined by analyzing aliquots of the reaction mixture at different times by analytical reverse-phase HPLC. To ensure equilibration between the vesicles, the samples were freeze-thawed every hour during the equilibration, using a dry ice-acetone bath for freezing and a bath sonicator during thawing, followed by sonication to clarity. The peptide/phospholipid ratios used varied between 1:100 and 1:1,500. In the case of DMPC bilayers, the equilibration reactions were also carried out above the thermal phase transition of the lipid (at 28°C) to ensure that the lipid was in the fluid phase (see Fig. 8, which is published as supporting information on the PNAS web site). After equilibration, the reactions were quenched by lowering the pH. The components of the equilibrium mixtures were analyzed by reverse-phase HPLC using an analytical C-4 column with a linear buffer A/buffer B gradient (A: 6:3:1 2-propanol/acetonitrile/water, 0.1% trifluoroacetic acid and B: water/0.1% trifluoroacetic acid). They typically consisted of a mixture of three species corresponding to the thiol-free peptide, mixed disulfide of peptide with GSH, and disulfide-bonded peptide. These species were identified by using matrix-assisted laser desorption ionization–time of flight MS. A small amount of the reaction mixture was used to determine the total free thiol content at the end of the reaction by using Ellman's reagent, 5,5′-dithiobis(2-nitrobenzoic acid). The amount of covalent dimer was calculated from the integrated HPLC peak areas of the present species in the chromatograms by using the software supplied with the HPLC.

For cholesterol concentration-dependence experiments, the peptide was incorporated into DLPC bilayers containing various amounts of cholesterol. The peptide/DPLC mole ratio was 1:500, and the final cholesterol concentration in the samples ranged between 1 and 25 mol percent (relative to lipid concentration). The ratio of GSSG to reduced GSH was 0.25.

Thermodynamic Analysis. The data obtained from thiol-disulfide exchange measurements (see Figs. 3 and 5) were analyzed according to Scheme 1, which illustrates the thermodynamic coupling between disulfide formation and tetramerization. This model is a simplified version of the more complex equilibria scheme we used previously (16).

In Scheme 1, the monomeric and tetrameric states are given as M and T, respectively, and their oxidation states are indicated as a subscript. The factor of 3 for the upper value of K_2 is related to the fact that a given Cys has three potential partners in the fully reduced tetramer, but only one in the half-oxidized structure. The present model does not include the disulfide-bonded dimeric species, D_{SS}, which was previously considered in the fitting model. The concentration of this species is very low under our experimental conditions, thus its contribution to the overall coupled equilibria is negligible. To fit the data, it was necessary to include a baseline correction, which presumably reflects the presence of some disulfide-bonded species insensitive to the redox potential of the solution. These species are generated because of a tendency of this peptide to form nonspecific aggregates. We found that these disulfide-bonded species are present in the system even under exclusively reducing conditions (incubation of the peptide incorporated into DLPC bilayers in DTT) and account for ≈18% of the total peptide.

Results

Incorporation of Peptides into Vesicles. The hydrophobic chain length of phospholipids controls the thickness of bilayers, which in turn frequently affects the activity of membrane proteins (27, 28). In general, native-like function requires a good match between the width of the apolar region of the bilayer and the hydrophobic length of the transmembrane helix. The peptide $M2TM_{19-46}$ has a 19-residue hydrophobic region spanning from residues 25 to 43. To determine how the chain length of the phospholipids affect the incorporation of this peptide into bilayers, it was incorporated into small unilamellar vesicles composed of DLPC, POPC, and DMPC. DLPC has an acyl chain length of 12 carbon atoms, DMPC has a chain length of 14 carbons, and POPC, the longest chain lipid investigated, contains mixed saturated/unsaturated chains with one double bond (16:0/18:1).

CD. The far-UV CD spectra of $M2TM_{19-46}$ incorporated into sonicated DLPC, DMPC, and POPC vesicles at a 1:500 peptide/lipid mole ratio and a peptide concentration of 50 μM, are shown in Fig. 9, which is published as supporting information on the PNAS web site. The spectra show that the peptide adopts an α-helical conformation when incorporated into lipid vesicles, as

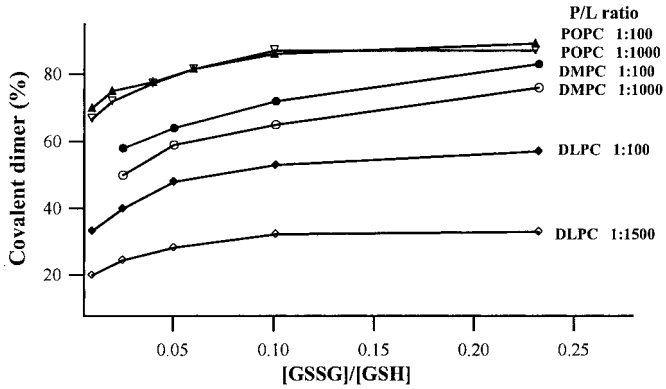

Fig. 1. Effect of the phospholipid acyl chain length on the covalent dimer formation. The peptide/phospholipid mole ratios (P/L) for each lipid investigated were as indicated. DMPC and DLPC show dependence on the P/L ratio, whereas POPC shows no dependence.

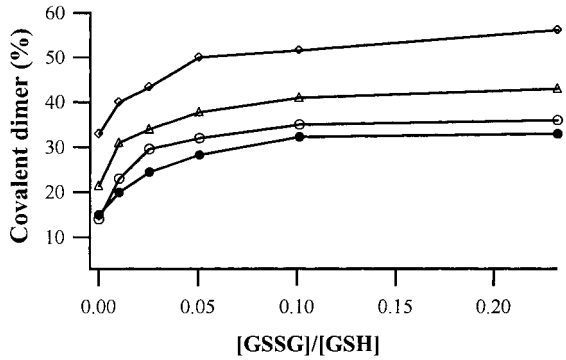

Fig. 2. Disulfide cross-linking in the presence of amantadine. ●, data without amantadine. The peptide/DLPC/amantadine mole ratios used were 1:1,500:5 (○), 1:1,500:15 (△), and 1:1,500:50 (◇).

indicated by the minima at 208 and 222 nm. These data confirm previous CD results reported in DMPC and DOPC vesicles for $M2TM_{22-46}$ (24) and earlier findings that this peptide is predominantly helical in lipid membranes (22). Previously, a relationship between the ellipticity ratio $\theta_{222}/\theta_{208}$ and the content of tetramer was established (26). Using this relationship, our data suggest that the stability of the tetramer follows POPC > DMPC > DLPC. This finding is consistent with the expectation that the width of the apolar region of the POPC bilayer would provide the best match for the length of the tetramer.

Effect of Lipid Chain Length on Reversible Disulfide Formation. To investigate further the effect of the bilayer thickness on the oxidation potential and tetramerization of $M2TM_{19-46}$ the peptide was studied in vesicles prepared from POPC, DMPC, and DLPC. The vesicles were incubated with GSH oxidized/reduced buffer and repeatedly annealed (see *Materials and Methods*) to assure equilibration of peptides between individual vesicles.

Because $M2TM_{19-46}$ exists in a reversible monomer–tetramer equilibrium, the redox behavior of the peptide should depend on the peptide/phospholipid ratio, becoming easier to oxidize as the fraction of tetramer increases with increasing peptide concentrations. The reduced form of $M2TM_{19-46}$ peptide was incorporated into vesicles at various peptide/phospholipid mole ratios, in the presence of GSH redox buffer containing known concentrations of GSSG and reduced GSH. The reaction was allowed to proceed to equilibrium and quenched by addition of HCl to effectively eliminate thiol exchange and oxidation, and the components present in the equilibrium mixture were separated and quantified by analytical RP-HPLC. The reversibility of the disulfide crosslinking process in DLPC bilayers was assessed by repeating the equilibration reactions, starting with the oxidized dimer rather than the reduced form of the peptide (see Fig. 10, which is published as supporting information on the PNAS web site). Irrespective of whether the initial starting material was oxidized or reduced, the same equilibrium distribution was observed.

Fig. 1 shows the extent of covalent dimer formed as a function of the redox potential and the phospholipid/peptide molar ratio in DLPC, DMPC, and POPC bilayers. At a given peptide/phospholipid molar ratio, the extent of disulfide formation follows the same trend observed by CD spectroscopy: POPC > DMPC > DLPC. Furthermore, the extent of covalent dimer formation indeed depends on the peptide/phospholipid ratio for DMPC and DLPC. By contrast, in POPC the curves were the same within experimental error at a molar ratio of 1:100 and 1:1,000. This behavior is consistent with the CD data, which suggested that the reduced peptide adopted a stable, fully tetrameric conformation in POPC vesicle, whereas it populated a significant fraction of both the monomeric and tetrameric aggregation states in DMPC and DLPC vesicles.

The data for POPC in Fig. 1 can be analyzed according to the model presented in Scheme 1. In POPC, the peptide should be fully tetrameric, allowing an evaluation of the oxidation potential in this state, by considering only the equilibria between the tetrameric species. Fitting of K_2 to the data for $M2TM_{19-46}$ in POPC, by the method of nonlinear least squares, indicates a value of 3.3 M. This equilibrium constant is often considered as an effective concentration of the Cys residues (29, 30) and is very close to the range of values typically observed for Cys residues in native folded proteins (5–20 M, although values as high as 1×10^5 M have been measured) (31–33).

To test the specificity of this process, we carried out the thiol-disulfide equilibrium assay in the presence of amantadine. Previously, it has been shown that $M2TM_{22-46}$ forms amantadine-sensitive ion channels in phospholipid bilayers (21), and amantadine binding favors tetramer formation (26). $M2TM_{19-46}$ peptide was incorporated into phospholipid vesicles at a low peptide/phospholipid mole ratio (1:1,500), and different amounts of amantadine were then added to these samples. Thiol-disulfide exchange was initiated by adding GSSG and GSH in varying ratios. Fig. 2 illustrates the enhancement in disulfide formation upon addition of amantadine. The shift in the curves is consistent with a shift in the monomer–tetramer equilibrium toward the tetrameric species, which is attributed to the preferential binding of amantadine to these species.

Quantitative Measurements of Peptide Association in Phospholipid Bilayers. Protein–protein interactions tend to be more specific and stronger in phospholipid environments as compared with detergent systems (34). To evaluate the dissociation constant for $M2TM_{19-46}$ tetramerization in phospholipid bilayers, we used the same procedure used in the quantitative measurement of association in detergent micelles (16). To obtain accurate measurements, the thiol-disulfide exchange equilibrium measurements were performed at a fixed GSSG/GSH ratio (0.25) and various peptide/phospholipid ratios. Fig. 3 shows the percent of covalent dimer formed as a function of peptide/phospholipid ratio. By curve-fitting the parameters shown in Scheme 1 to the data, a value of 5.0×10^{-9} MF^3 (MF is the mole fraction of peptide in the phospholipid bilayer) was derived for the tetrameric dissociation constant. A comparison with the value obtained from thiol-disulfide exchange measurements in detergent micelles (5.0×10^{-7} MF^3) indicates that the association is 2 orders of magnitude tighter in DLPC than in detergent environments and even tighter than this value in DMPC and POPC bilayers. These values of the tetrameric dissociation

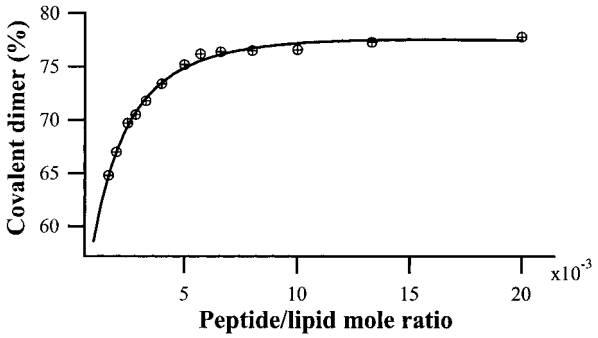

Fig. 3. Calculated percent of covalent dimer as a function of peptide/DLPC ratio. Thiol-disulfide exchange equilibrations were performed at a GSSG/GSH ratio of 0.25. The solid line is the best fit to the data as described in the text.

constants assume peptides can freely reorient in bilayers and micelles. If, as is likely the case, peptides in bilayers cannot reorient and moreover, are equally distributed in each orientation, the dissociation constant in bilayers should be divided by 8 (2^3) for a fair comparison. The tighter association of $M2TM_{19-46}$ in phospholipid bilayers compared with that in detergent micelles is in accord with the observations that phospholipid environments can considerably stabilize membrane proteins.

Effect of Cholesterol on the Tetramerization Equilibrium. The data presented above indicate that the thickness of the host phospholipid bilayer controls the association of the peptide. An alternative method to modulate membrane thickness is the addition of cholesterol. Numerous studies have shown that cholesterol affects the behavior of membrane inserted helices and the function of many membrane-associated proteins directly or by means of its effect on the physical properties of the phospholipid bilayer, i.e., bilayer hydrophobic thickness and material moduli (35–42). For example, cholesterol can stabilize α-helices in membrane proteins (43, 44); it also affects the function of many membrane proteins (36, 39, 45–48) and can alter ion channel gating (49–51).

Therefore, we examined how cholesterol influences the $M2TM_{19-46}$ association in DLPC bilayers. Addition of cholesterol to the DLPC bilayers is expected to result in an increase of the bilayer thickness, which should favor the formation of tetramers. Fig. 4 shows the cholesterol-induced effect on the association of $M2TM_{19-46}$. At two peptide/phospholipid ratios, enhancement of the disulfide formation is observed for samples containing 15 mol

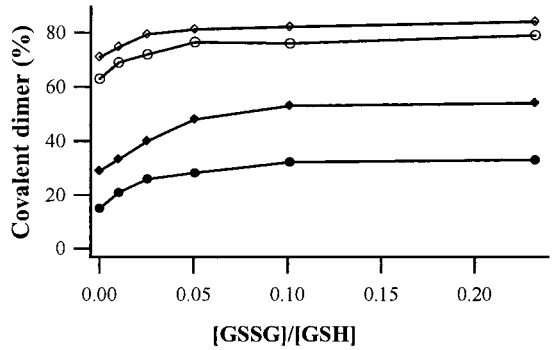

Fig. 4. Disulfide cross-linking in the presence of cholesterol. The peptide was incorporated into DLPC bilayers at peptide/phospholipid mole ratios of 1:1,500 (●) and 1:100 (◆). The data obtained upon addition of cholesterol to these samples are shown as ○ (1:1,500 peptide/DLPC sample plus 15 mol percent cholesterol) and ◇ (1:100 peptide/DLPC sample plus 15 mol percent cholesterol).

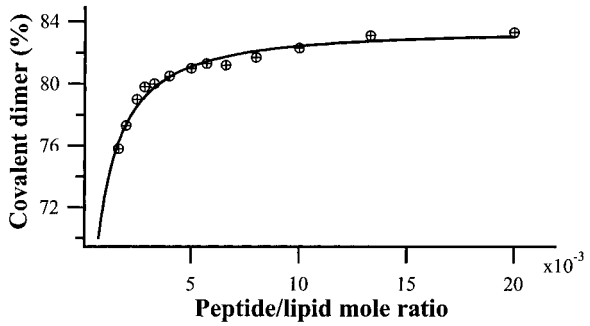

Fig. 5. Quantitative measurements of association in the presence of cholesterol. The calculated percent of covalent dimer is plotted as a function of peptide/DLPC ratio. $M2TM_{19-46}$ was incorporated into DLPC bilayers containing 7 mol percent cholesterol at various peptide/phospholipid ratios. Thiol-disulfide exchange equilibrations were performed at a GSSG/GSH ratio of 0.25. The solid line is the best fit to the data as described in the text.

percent of cholesterol relative to samples lacking cholesterol. In the presence of cholesterol the curves are very similar to those observed in POPC, indicative of very strong stabilization of the tetramer.

To obtain a better estimate of the extent to which cholesterol affects the energetics of assembly, the thiol-disulfide exchange reactions were measured as a function of the peptide/phospholipid ratio in DLPC bilayers with or without 7 mol percent cholesterol (Fig. 5). The dissociation constant for the tetramerization interaction was found to be ≈10-fold lower in the presence of 7 mol percent cholesterol, which is indicative of a tighter association of $M2TM_{19-46}$ in the presence of cholesterol.

The above data are consistent with the prediction that increasing the bilayer width by the addition of cholesterol would increase the stability of the tetramer. However, cholesterol is also known to affect the properties of membrane proteins through specific binding effects. To help distinguish between these two possibilities, we examined the cholesterol dependence of thiol-disulfide exchange in DLPC bilayers. Fig. 6 indicates that the association of $M2TM_{19-46}$ increases markedly with respect to the cholesterol levels in the phospholipid bilayer, consistent with our expectation that cholesterol increases the association by modulating the width of the bilayer. From these data, it is possible to obtain a value of the observed dissociation constant for tetramerization ($K_{obs,}$ computed according to Scheme 1) at various cholesterol concentrations. We then ask whether the variation in this parameter with respect to the concentration of cholesterol is more consistent with the site-binding model. Fig. 7 illustrates the value of K_{obs} as a function of cholesterol concentration. The curve associated with the data represents the

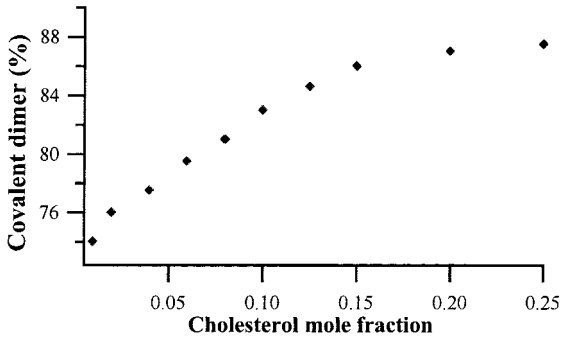

Fig. 6. Effect of increasing the mole fraction of cholesterol on the extent of disulfide cross-linking. The peptide/phospholipid mole ratio was 1:500, and the thiol-disulfide exchange equilibrations were performed at a GSSG/GSH ratio of 0.25.

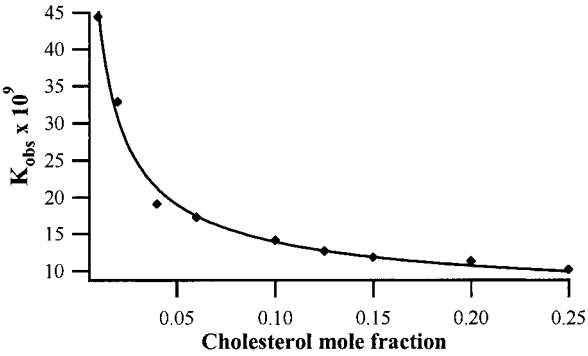

Fig. 7. Effect of cholesterol mole fraction on the observed tetramerization constant (K_{obs}). The solid line represents the best fit to the data as described in the text.

best fit to a specific cholesterol binding model, which is described in Scheme 2, which is published as supporting information on the PNAS web site. Although a good fit can be obtained, the limiting stoichiometry is ≈0.6 molecules cholesterol bound per tetramer, a value that is physically unreasonable. Thus, it is most likely that the observed effects of cholesterol on the association follow from changes in the phospholipid bilayer physical properties (i.e., membrane width) and not from a specific high-affinity binding of cholesterol to the protein.

Discussion

An initial goal of this study was to establish a method for quantitative measurements of the thermodynamics of peptide association in phospholipid bilayers. Thiol-disulfide equilibrium measurements in phospholipid bilayers indicate that the redox behavior of $M2TM_{19-46}$ peptide depends on the peptide/phospholipid ratio. The specificity of the disulfide bonding process in phospholipid bilayers was demonstrated in the presence of amantadine. Disulfide formation depends on the phospholipid bilayer thickness, as assessed by altering the width of the phospholipid bilayer by varying the phospholipid acyl chain length or by inclusion of cholesterol. An enhanced disulfide bonding was observed upon increasing the width of the bilayer, suggesting that significant interactions occur between helices leading to a tight association of the peptide into tetramers in response to the increased bilayer thickness. These results are in line with previous reports of self-association of peptides as an adjustment response to variations in the bilayer thickness (52, 53). Extensive studies have shown that hydrophobic mismatch (the difference between the hydrophobic length of peptide and membrane) affects protein activity (54–56), may trigger protein aggregation, helix tilt, and changes in backbone conformation (52, 53, 57–59), and affect the phospholipid structure and organization (53, 60, 61). It is, however, important to note that the presence of a double bond in POPC and the introduction of cholesterol into a saturated lipid could introduce packing defects that may be important in peptide association.

The approximate widths of the apolar (fatty acyl) regions of the phophatidylcholine bilayers investigated are: DLPC, 19.5 Å (62); DMPC, 23.0 Å (27); and POPC, 26.5 Å (27). These values can be compared with the hydrophobic length of $M2TM_{19-46}$ (sequence: C^{19}NDSSDP^{25}LVVAASIIGILHLILWIL^{43}DRL), calculated for the hydrophobic core of the peptide, Pro-25–Leu-43 sequence, corresponding to the transmembrane region. Assuming an ideal α-helical conformation and using a helix translation of 1.5 Å per residue for a hydrophobic stretch of 19 residues, the peptide length was calculated to be ≈28.5 Å. Given this value, the length of the peptide matches more closely the hydrophobic width of the POPC bilayers and exceeds the hydrophobic thickness of DMPC and DLPC bilayers. Thus, a mismatch between peptide hydrophobic length and bilayer thickness is expected to occur with the shorter chain phospholipids.

It is interesting to note that many models have been proposed for the orientation of the M2 transmembrane helix in membranes. Some predict an angle as large as 40° between the helical axis and the bilayer normal (24, 63–65). This angle would translate to a length of 21.8 Å [28.5*cos(40°)], which is difficult to reconcile with our data. Instead, a less acute angle would be more consistent with the observed preference for POPC bilayers.

Cholesterol plays a key role in membrane organization, function, and sorting (39, 66–68). Numerous studies have demonstrated that cholesterol interacts preferentially with membrane lipids (40) and proteins (69) and is an important factor in lipid raft formation and assembly (68, 70–74). Rafts are postulated to participate in important cellular processes, such as protein trafficking (37, 72, 75) and signal transduction events (70, 76–78). Our data allow an estimation of the magnitude of the energies involved in the preferential transfer of specific membrane proteins from a cholesterol-poor to a cholesterol-rich phase. By consideration of thermodynamic cycles, it is possible to determine the $\Delta\Delta G_{tr}$ for the transfer of the tetrameric form of M2 to a cholesterol-rich phase, relative to the corresponding value for the monomeric form of the peptide (Scheme 3, which is published as supporting information on the PNAS web site). Furthermore, analysis of the data in Fig. 6 indicates that $\Delta\Delta G_{tr}$ depends approximately linearly with respect to the concentration of cholesterol. Extrapolation of these data to 50% cholesterol (the approximate concentration of cholesterol in lipid rafts) indicates that $\Delta\Delta G_{tr}$ is on the order of 8.6 kcal/mol, corresponding to an ≈10^6-fold preference for the transfer of the tetrameric species. This is a crude estimation because of the long extrapolation and the requirement of additional studies with more relevant phospholipids to determine the magnitude of the corresponding effect *in vivo*. Nevertheless, this result illustrates the magnitude of the effect that cholesterol can have on the transfer (sorting) of a protein into lipid rafts.

In summary, these studies demonstrate that the disulfide-coupled equilibria method can be successfully applied to thermodynamic measurements of membrane protein association in phospholipid bilayers. Although disulfide interchange reactions have been the subject of previous studies (79–85), there are no previous reports, to our knowledge, on the use of a disulfide coupled-folding approach to measure the energetics of reversible transmembrane peptide association in phospholipid bilayers. The development of experimental methods to study the folding in phospholipid environments holds great promise for providing detailed insights into the understanding of the membrane protein folding process.

This work was supported by National Institutes of Health Grant GM 54623.

1. White, S. H. & Wimley, W. C. (1999) *Annu. Rev. Biophys. Biomol. Struct.* **28,** 319–365.
2. Jordan, P., Fromme, P., Witt, H. T., Klukas, O., Saenger, W. & Krauss, N. (2001) *Nature* **411,** 909–917.
3. Arora, A., Abildgaard, F., Bushweller, J. H. & Tamm, L. K. (2001) *Nat. Struct. Biol.* **8,** 334–338.
4. Locher, K. P., Lee, A. T. & Rees, D. C. (2002) *Science* **296,** 1091–1098.
5. Bass, R. B., Strop, P., Barclay, M. & Rees, D. C. (2002) *Science* **298,** 1582–1587.
6. Dutzler, R., Campbell, E. B., Cadene, M., Chait, B. T. & MacKinnon, R. (2002) *Nature* **415,** 287–294.
7. Jiang, Y., Lee, A., Chen, J., Cadene, M., Chait, B. T. & MacKinnon, R. (2002) *Nature* **30,** 515–522.
8. Jiang, Y., Lee, A., Chen, J., Cadene, M., Chait, B. T. & MacKinnon, R. (2002) *Nature* **30,** 523–526.
9. Fisher, L. E., Engelman, D. M. & Sturgis, J. N. (1999) *J. Mol. Biol.* **293,** 639–651.

10. Adair, B. D. & Engelman, D. M. (1994) *Biochemistry* **33,** 5539–5544.
11. Choma, C., Gratkowski, H., Lear, J. D. & DeGrado, W. F. (2000) *Nat. Struct. Biol.* **7,** 161–166.
12. Fleming, K. G., Ackerman, A. L. & Engelman, D. M. (1997) *J. Mol. Biol.* **272,** 266–275.
13. Howard, K. P., Lear, J. D. & DeGrado, W. F. (2002) *Proc. Natl. Acad. Sci. USA* **99,** 8568–8572.
14. Gratkowski, H., Lear, J. D. & DeGrado, W. F. (2001) *Proc. Natl. Acad. Sci. USA* **98,** 880–885.
15. DeGrado, W., Gratkowski, H. & Lear, J. (2003) *Protein Sci.* **12,** 647–665.
16. Cristian, L., Lear, J. D. & DeGrado, W. F. (2003) *Protein Sci.* **12,** 1732–1740.
17. Holsinger, L. J. & Lamb, R. A. (1991) *Virology* **183,** 32–43.
18. Pinto, L. H., Holsinger, L. J. & Lamb, R. A. (1992) *Cell* **69,** 517–528.
19. Wang, C., Takeuchi, K., Pinto, L. H. & Lamb, R. A. (1993) *J. Virol.* **67,** 5585–5594.
20. Sakaguchi, T., Tu, Q., Pinto, L. H. & Lamb, R. A. (1997) *Proc. Natl. Acad. Sci. USA* **94,** 5000–5005.
21. Duff, K. C. & Ashley, R. H. (1992) *Virology* **190,** 485–489.
22. Duff, K. C., Kelly, S. M., Price, N. C. & Bradshaw, J. P. (1992) *FEBS Lett.* **311,** 256–258.
23. Kovacs, F. & Cross, T. A. (1997) *Biophys. J.* **73,** 2511–2517.
24. Kovacs, F., Denny, J. K., Song, Z., Quine, J. R. & Cross, T. A. (2000) *J. Mol. Biol.* **295,** 117–125.
25. Kochendoerfer, G. G., Salom, D., Lear, J. D., Wilk-Orescan, R., Kent, S. B. H. & DeGrado, W. F. (1999) *Biochemistry* **38,** 11905–11913.
26. Salom, D., Hill, B. R., Lear, J. D. & DeGrado, W. F. (2000) *Biochemistry* **39,** 14160–14170.
27. Lewis, B. A. & Engelman, D. M. (1983) *J. Mol. Biol.* **166,** 211–217.
28. Caffrey, M. & Feigenson, G. W. (1981) *Biochemistry* **20,** 1949–1961.
29. Creighton, T. E. (1986) *Methods Enzymol.* **131,** 83–106.
30. Creighton, T. E. (1983) *Biopolymers* **22,** 49–58.
31. Lin, T. Y. & Kim, P. S. (1989) *Biochemistry* **28,** 5282–5287.
32. Regan, L., Rockwell, A., Wasserman, Z. & DeGrado, W. F. (1994) *Protein Sci.* **3,** 2419–2427.
33. Creighton, T. E. & Goldenberg, D. P. (1984) *J. Mol. Biol.* **179,** 497–526.
34. Haltia, T. & Freire, E. (1995) *Biochim. Biophys. Acta* **1228,** 1–27.
35. Nezil, F. A. & Bloom, M. (1992) *Biophys. J.* **61,** 1176–1183.
36. Cornelius, F. (2001) *Biochemistry* **27,** 8842–8851.
37. Bretscher, M. S. & Munro, S. (1993) *Science* **261,** 1280–1281.
38. Ren, J., Lew, S., Wang, Z. & London, E. (1997) *Biochemistry* **36,** 10213–10220.
39. Yeagle, P. L. (1985) *Biochim. Biophys. Acta* **822,** 267–287.
40. McMullen, T. P. W. & McElhaney, R. N. (1996) *Curr. Opin. Colloid Interface Sci.* **1,** 83–90.
41. Needham, D. & Nunn, R. (1990) *Biophys. J.* **58,** 997–1009.
42. Lundbaek, J., Andersen, O., Werge, T. & Nielsen, C. (2003) *Biophys. J.* **84,** 2080–2089.
43. Fong, T. & McNamee, M. (1986) *Biochemistry* **25,** 830–840.
44. Rooney, M., Lange, Y. & Kauffman, J. (1984) *J. Biol. Chem.* **259,** 8281–8285.
45. Silvius, J. R., McMillen, D. A., Saley, N. D., Jost, P. C. & Griffith, O. H. (1984) *Biochemistry* **23,** 538–547.
46. Schubert, D. & Boss, K. (1982) *FEBS Lett.* **150,** 4–8.
47. Simmonds, A., Rooney, E. & Lee, A. (1984) *Biochemistry* **23,** 1432–1441.
48. Yeagle, P., Young, J. & Rice, D. (1988) *Biochemistry* **27,** 6449–6452.
49. Schindler, H. (1982) *Neurosci. Res. Progr. Bull.* **20,** 295–301.
50. Romanenko, V., Rothblat, G. & Levitan, I. (2002) *Biophys. J.* **83,** 3211–3222.
51. Chang, H., Reitstetter, R., Mason, R. & Gruener, R. (1995) *J. Membr. Biol.* **143,** 51–63.
52. Ren, J., Lew, S., Wang, J. & London, E. (1999) *Biochemistry* **38,** 5905–5912.
53. Killian, J. A. (1998) *Biochim. Biophys. Acta* **1376,** 401–416.
54. Froud, R. J., Earl, C. R. A., East, J. M. & Lee, A. G. (1986) *Biochim. Biophys. Acta* **860,** 354–360.
55. Lee, A. G. (1998) *Biochim. Biophys. Acta* **1376,** 381–390.
56. Carruthers, A. & Melchior, D. L. (1988) *Annu. Rev. Physiol.* **50,** 257–271.
57. Harzer, U. & Bechinger, B. (2000) *Biochemistry* **39,** 13106–13114.
58. DePlanque, M. R. R., Goormaghtigh, E., Greathouse, D. V., Koeppe, R. E., Kruijtzer, J. A. W., Liskamp, R. M. J., DeKruijff, B. & Killian, J. A. (2001) *Biochemistry* **40,** 5000–5010.
59. Webb, R. J., East, J. M., Sharma, R. P. & Lee, A. G. (1998) *Biochemistry* **37,** 673–679.
60. Dumas, F., Lebrun, M. C. & Tocanne, J. F. (1999) *FEBS Lett.* **458,** 271–277.
61. Mouritsen, O. G. & Bloom, M. (1993) *Annu. Rev. Biophys. Biomol. Struct.* **22,** 145–171.
62. Silvius, J. R. (1982) *Thermotropic Phase Transitions of Pure Lipids in Model Membranes and Their Modifications by Membrane Proteins* (Wiley, New York).
63. Zhong, Q., Newbs, D., Pattnaik, P., Lear, J. & Klein, M. (2000) *FEBS Lett.* **473,** 195–198.
64. Wang, J., Kovacs, F. & Cross, T. A. (2001) *Protein Sci.* **10,** 2241–2250.
65. Forrest, L. R., Kukol, A., Arkin, I. T., Tieleman, D. P. & Sanson, M. S. P. (2000) *Biophys. J.* **78,** 55–69.
66. Fielding, C. J. & Fielding, P. E. (1997) *J. Lipid Res.* **38,** 1503–1520.
67. Liscum, L. & Munn, N. J. (1999) *Biochim. Biophys. Acta* **1438,** 19–37.
68. Simons, K. & Ikonen, E. (2000) *Science* **290,** 1721–1726.
69. Gimpl, G., Burger, K. & Fahrenholz, F. (1997) *Biochemistry* **36,** 10959–10974.
70. Brown, D. & London, E. (1998) *Annu. Rev. Cell Dev. Biol.* **14,** 111–136.
71. Brown, D. A. & London, E. (2000) *J. Biol. Chem.* **275,** 17221–17224.
72. Simons, K. & Ikonen, E. (1997) *Nature* **387,** 569–572.
73. Mukherjee, S. & Maxfield, F. (2000) *Traffic* **1,** 203–211.
74. Jacobson, K. & Dietrich, C. (1999) *Trends Cell Biol.* **9,** 87–91.
75. Ikonen, E. (2001) *Curr. Opin. Cell Biol.* **13,** 470–477.
76. Incardona, J. P. & Eaton, S. (2000) *Curr. Opin. Cell Biol.* **12,** 193–203.
77. Moffet, S., Brown, D. & Linder, M. (2000) *J. Biol. Chem.* **275,** 2191–2192.
78. Baird, B., Sheets, E. & Holowka, D. (1999) *Biophys. Chem.* **82,** 109–119.
79. Erlanson, D., Braisted, A., Raphael, D., Randal, M., Stroud, R., Gordon, E. & Wells, J. (2000) *Proc. Natl. Acad. Sci. USA* **97,** 9367–9372.
80. Blandl, T., Cochran, A. G. & Skelton, N. J. (2003) *Protein Sci.* **12,** 237–247.
81. Cochran, A. G., Tong, R. T., Starovasnik, M. A., Park, E. J., McDowell, R. S., Theaker, J. E. & Skelton, N. J. (2001) *J. Am. Chem. Soc.* **123,** 625–632.
82. McClain, D. L., Woods, H. L. & Oakley, M. G. (2001) *J. Am. Chem. Soc.* **123,** 3151–3152.
83. Davidson, M. K. S. & Regen, S. L. (1997) *Chem. Rev.* **97,** 1269–1279.
84. Sugahara, M., Uragami, M. & Regen, S. L. (2002) *J. Am. Chem. Soc.* **124,** 4253–4256.
85. Regen, S. L. (2002) *Curr. Opin. Chem. Biol.* **6,** 729–735.